

# Sperm-borne microRNA-34c is required for the first cleavage division in mouse

Wei-Min Liu<sup>a,b,1</sup>, Ronald T. K. Pang<sup>a,b,1</sup>, Philip C. N. Chiu<sup>a,b</sup>, Benancy P. C. Wong<sup>a</sup>, Kaiqin Lao<sup>c</sup>, Kai-Fai Lee<sup>a,b</sup>, and William S. B. Yeung<sup>a,b,2</sup>

<sup>a</sup>Department of Obstetrics and Gynaecology and <sup>b</sup>Centre for Reproduction, Development and Growth, University of Hong Kong, Pokfulam, Hong Kong, People's Republic of China; and <sup>c</sup>Applied Biosystems, Foster City, CA 94404

Edited by Victor R. Ambros, University of Massachusetts Medical School, Worcester, MA, and approved December 2, 2011 (received for review June 27, 2011)

In mammals, the sperm deliver mRNA of unknown function into the oocytes during fertilization. The role of sperm microRNAs (miRNAs) in preimplantation development is unknown. miRNA profiling identified six miRNAs expressed in the sperm and the zygotes but not in the oocytes or preimplantation embryos. Sperm contained both the precursor and the mature form of one of these miRNAs, miR-34c. The absence of an increased level of miR-34c in zygotes derived from  $\alpha$ -amanitin-treated oocytes and in parthenogenetic oocytes supported a sperm origin of zygotic miR-34c. Injection of miR-34c inhibitor into zygotes inhibited DNA synthesis and significantly suppressed first cleavage division. A 3' UTR luciferase assay and Western blotting demonstrated that miR-34c regulates B-cell leukemia/lymphoma 2 (Bcl-2) expression in the zygotes. Coinjection of anti-Bcl-2 antibody in zygotes partially reversed but injection of Bcl-2 protein mimicked the effect of miR-34c inhibition. Oocyte activation is essential for the miR-34c action in zygotes, as demonstrated by a decrease in 3' UTR luciferase reporter activity and Bcl-2 expression after injection of precursor miR-34c into parthenogenetic oocytes. Our findings provide evidence that sperm-borne miR-34c is important for the first cell division via modulation of Bcl-2 expression.

During fertilization, a sperm contributes more than just the paternal genome to the resulting zygote. Phospholipase C $\zeta$  and postacrosomal sheath WW domain-binding protein of the sperm initiate calcium signaling crucial to oocyte activation (1) and promote meiotic resumption and pronuclear formation (2). Mammalian sperm contain an array of RNAs including mRNA and microRNA (miRNA) (3). Some of these RNAs are delivered to the oocyte during fertilization (4). Although they are implicated in mediating epigenetic inheritance in mouse (5), their roles in fertilization and/or early embryonic development remain unknown.

Accumulating evidence shows that miRNAs are critical in controlling key developmental events; however, the role of miRNAs in the development of early preimplantation embryos is controversial. The dynamic changes in the expression of miRNAs in preimplantation embryos (6–8) and the increased synthesis of miRNAs after the two-cell stage in mouse embryos (7, 9) suggest that miRNAs have a functional role in the preimplantation period. This evidence is supported by the observations that mouse oocytes without the miRNA-processing enzyme *Dicer* have a minimal amount of miRNA, that their resulting zygotes cannot pass through the first cleavage division (7), and that *Dicer*-null embryos carrying maternal *dicer* die at embryonic day 7.5 (E7.5) (10). On the other hand, knockout of DiGeorge syndrome critical region gene 8 (*Dgcr8*), another key miRNA-processing enzyme, produces normal blastocysts (11), although embryonic arrest occurs at E6.5 (12). These observations together with the suppressive state of miRNA function in mouse oocytes (11, 13), suggest that miRNA is dispensable in early embryos. However, these latter reports (11–13) did not study the possible involvement of sperm-borne miRNA in early embryos, which is addressed in the present study.

## Results

**Mouse Zygotes Possess miRNAs Expressed in Sperm but Not in Oocytes.** miRNA expression profiles were determined by a multiplex quan-

titative real-time PCR (qRT-PCR) approach (7). Of the 238 miRNAs studied, 163 were detected in the preimplantation embryos. Hierarchical clustering analysis showed a pattern of dynamic miRNA expression in early development (Fig. 1A and Dataset S1). The total amount of miRNA increased continuously from the four-cell embryo to the blastocyst stage (Fig. S1A), consistent with miRNA synthesis in early embryogenesis (6–8).

*k*-means Pearson correlation clustering identified 94 differentially expressed miRNAs in the embryos ( $P < 0.05$ ; one-way ANOVA). They were grouped into six clusters according to their expression pattern (Fig. 1B, Table S1, and Fig. S1B). Cluster 1 consisted of 16 miRNAs that were up-regulated at the zygote stage but decreased thereafter. Independent qRT-PCRs on the total RNA isolated from five oocytes or embryos without pre-PCR amplification showed that the expression patterns of miR-34c, -145, and -196b (Fig. 1B and Fig. S1C) relative to that of miR-16, which did not change significantly in the preimplantation period, were similar to that obtained by the multiplex approach, confirming the reliability of the miRNA profiles obtained.

Epididymal sperm contain both mature and immature sperm. To study the miRNAs in sperm with fertilization potential, we incubated sperm with zona pellucida of oocytes and collected the zona-bound sperm. Zona pellucida binding is predictive of sperm fertilizing capacity in humans. The miRNA expression profile of the zona-bound sperm (Fig. 1A and Dataset S1) showed that only 25 miRNAs were expressed at levels twofold higher than the detection limit of the assay (Table S1). Six miRNAs (miR-34b, -34c, -99a, -214, -451, and -449) also were found in one-cell embryos but not in the oocytes or in embryos beyond the one-cell stage. MiR-34c was chosen for further study because it is highly expressed in the mouse round spermatids (14).

**Zygotic miR-34c Is Derived from Sperm.** The level of miR-34c in a sperm as determined by qRT-PCR was comparable to that in a zygote (Fig. 1C). Oocytes contained an undetectable amount of miR-34c. Because miRNAs must be incorporated into a complex containing argonaute protein 2 (Ago2) for functioning, we captured functional miR-34c in sperm by coimmunoprecipitation with Ago2 and compared the results with normal rabbit IgG and no-antibody controls. The results showed that miR-34c was highly enriched in the Ago2-bound fraction (Fig. 1D).

We determined whether sperm-borne miRNA could be delivered to the zygote by transduction of the precursor of miR-212 into sperm. This miRNA was chosen because its mature form is

Author contributions: W.-M.L., R.T.K.P., and W.S.B.Y. designed research; W.-M.L., R.T.K.P., P.C.N.C., and B.P.C.W. performed research; P.C.N.C. and K.L. contributed new reagents/analytic tools; W.-M.L., R.T.K.P., and K.-F.L. analyzed data; and W.-M.L., R.T.K.P., and W.S.B.Y. wrote the paper.

The authors declare no conflict of interest.

This article is a PNAS Direct Submission.

<sup>1</sup>W.-M.L. and R.T.K.P. contributed equally to the work.

<sup>2</sup>To whom correspondence should be addressed. E-mail: wsbyeung@hku.hk.

This article contains supporting information online at [www.pnas.org/lookup/suppl/doi:10.1073/pnas.1110368109/-DCSupplemental](http://www.pnas.org/lookup/suppl/doi:10.1073/pnas.1110368109/-DCSupplemental).

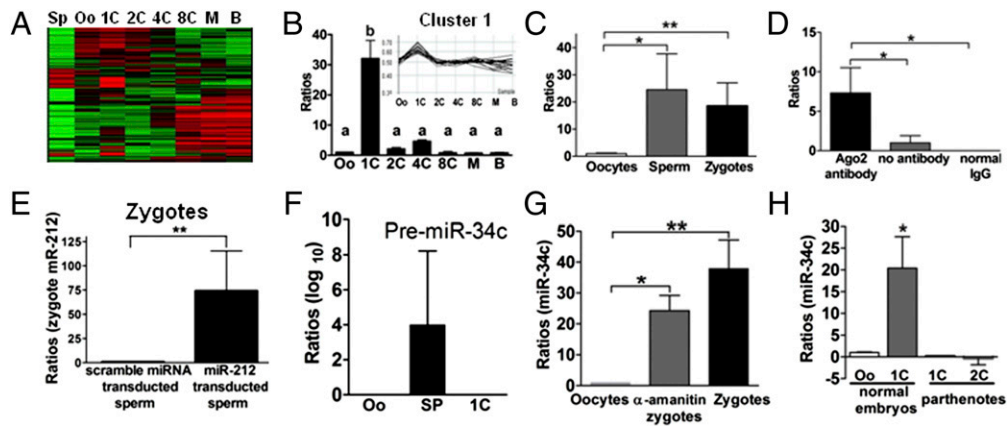


**Fig. 1.** miRNA expression in gametes and preimplantation embryos. (A) Supervised hierarchical clustering of miRNA expression. The heat map represents normalized, log-transformed relative intensities for miRNA in sperm (SP), oocyte (Oo), one-cell (1C), two-cell (2C), four-cell (4C), eight-cell (8C), morula (M), and blastocyst (B) stages. Red, green, and black colors represent high, low, and mean expression levels of miRNAs, respectively. (B) Expression pattern of cluster 1 miRNAs and miR-34c expression determined by qRT-PCR without preamplification on pooled embryos ( $n = 5$ ). All values were calculated against cycle threshold (Ct) values of oocytes and are presented as relative fold-change against oocyte miRNAs [ $2^{-(Ct_{\text{oocyte}} - Ct_x)}$ ]. All data were normalized by endogenous RNA U6 expression. The letters "a" and "b" above bars denote  $P < 0.05$ . (C) Expression of miR-34c in oocytes, sperm, and zygotes as determined by qRT-PCR ( $n = 4$ ). Five sperm, oocytes, or zygotes were used in each experiment. (D) Expression of miR-34c in Ago2 complex of sperm. Data are presented as relative to the no-antibody control. (E) Zygotes fertilized with miR-212 precursor-transduced sperm had significantly higher levels of mature miR-212 than zygotes fertilized with scramble miRNA precursor-loaded sperm ( $n = 3$ ). (F) MiR-34c precursor (Pre-miR-34c) was detected only in sperm but not in oocytes and zygotes, as determined by qRT-PCR. (G) miR-34c expression was significantly higher in zygotes and in  $\alpha$ -amanitin-treated oocytes than in nontreated oocytes ( $n = 3$ ). (H) Expression of miR-34c was significantly higher in one-cell zygotes (1C) than in oocytes (Oo) or in one-cell (1C) and two-cell (2C) parthenotes 11 h after ethanol activation. \* $P < 0.05$ ; \*\* $P < 0.001$ .

absent in sperm. The precursor form was transduced to determine the ability of zygotes to process miRNAs. A qRT-PCR assay that detected only mature miR-212 showed that in vitro-fertilized zygotes derived from the sperm loaded with precursor miR-212 contained more mature miR-212 than zygotes inseminated with control sperm with scramble precursor (Fig. 1E), indicating that precursor miRNA in sperm can be delivered to and be converted into mature form in the zygotes.

qRT-PCR showed that only the sperm, not the oocytes and zygotes, contained precursor miR-34c (Fig. 1F). To eliminate the possibility that the zygotes transcribed precursor miR-34c that was converted rapidly into the mature form, we compared the expression of miR-34c in zygotes derived from oocytes treated with the transcription inhibitor  $\alpha$ -amanitin. The treatment could not prevent the increase of miR-34c in zygotes, consistent with a sperm origin of zygotic miR-34c (Fig. 1G). The conclusion was supported further by the absence of miR-34c in ethanol-activated oocytes (Fig. 1H).

**MiR-34c Is Involved in the First Cleavage.** The hypothesis that the zygotic increase in miR-34c is related to the first cleavage was tested by injecting a miR-34c inhibitor into the zygotes 21 h after the injection of human chorionic gonadotropin (hCG). More than 70% of the zygotes injected with the miR-34c inhibitor failed to cleave, whereas more than 97% of the zygotes injected with the scramble inhibitor cleaved (Fig. 2A). In 80% of the arrested zygotes injected with miR-34c inhibitor, the pronuclei did not fuse even 20 h after injection (Fig. 2B).

The BrdU incorporation assay showed that only 38% of the zygotes injected with the miR-34c inhibitor had DNA synthesis, whereas 87% of those receiving the scramble inhibitor contained the signal (Fig. 2C). However, injection of the miR-34c inhibitor 30 h after hCG injection, when DNA synthesis of the zygotes had been completed (15), did not affect the first cell division; more than 95% of the injected zygotes in both groups formed two-cell embryos.

**Bcl-2 Is a Target Gene of miR-34c in Zygotes.** *In silico* prediction (TargetScan; [www.targetscan.org](http://www.targetscan.org)) indicated Bcl-2 as a target gene

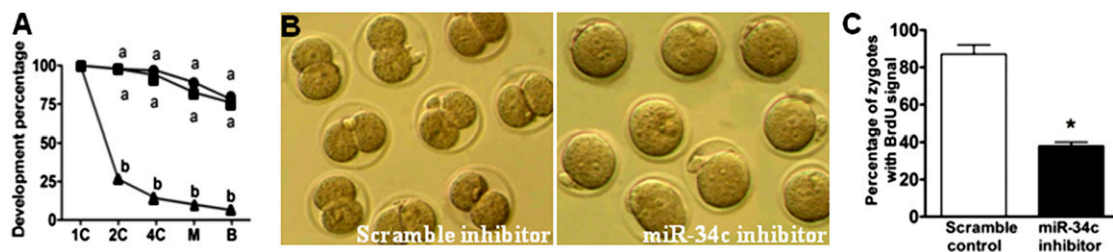


**Fig. 2.** Effects of miR-34c inhibitor on development of mouse embryos. (A) Injection of the miR-34c inhibitor suppressed zygote development ( $n = 5$ ). Percentage of development is based on the number of one-cell embryos (1C) used. There were significant decreases in the development at two-cell (2C), four-cell (4C), morula (M), and blastocyst (B) stages derived from zygotes injected with the miR-34c inhibitor ( $\blacktriangle$ ) compared with control zygotes injected with the scramble inhibitor ( $\blacksquare$ ). No difference in development was found between the untreated ( $\bullet$ ) and the control zygotes. Each data point represents more than 200 embryos. The letters "a" and "b" denote  $P < 0.001$  at the same time point. (B) The MiR-34c inhibitor inhibited pronuclei fusion. The pronuclei in zygotes injected with scramble inhibitor fused, and the zygotes cleaved 20 h after injection (magnification: 10 $\times$ ). (C) The percentage of embryos expressing BrdU signals was significantly lower after the injection of miR-34c inhibitor than after the injection of scramble inhibitor ( $n = 3$ ). \* $P < 0.05$  with the scramble inhibitor.

of miR-34c (Fig. 3A). In JAR cells, treatment with an miR-34c inhibitor for 24 h significantly increased the luciferase signal in the 3' UTR functional assay and Bcl-2 protein expression (Fig. 3B and C). In zygotes, the expression of Bcl-2 protein 6 h after injection of an miR-34c inhibitor also was increased significantly compared with the scramble-injected control (Fig. 3D). A short treatment was used for the zygotes because control zygotes cleaved with longer incubation.

**Bcl-2 Mediates the Inhibitory Effect of miR-34c on First Cleavage.** Similar to treatment with the miR-34c inhibitor, injection of Bcl-2 protein into zygotes inhibited the first cleavage (Fig. 4A). Coinjection of the miR-34c inhibitor and anti-Bcl-2 antibody partially nullified the effect of the inhibitor (Fig. 4B), confirming that Bcl-2 partly mediates the effect of miR-34c inhibitor. Injection of the anti-Bcl-2 antibody alone did not affect zygotic division. Treatment with the miR-34c inhibitor also elevated p27 expression (Fig. 4C). Examination of other potential miR-34c target genes found that miR-34c inhibitor increased c-myc expression but not the expression of cAMP-responsive element-binding (CREB). The other potential target, E2F3, was undetectable (Fig. S2).

**Activation Relieves the Suppressive State of Oocytes on miRNA Function.** Injection of precursor miR-34c into oocytes did not affect the expression of Bcl-2 protein and the Bcl-2 3' UTR reporter activities (Fig. 5A), confirming that the biological activities of miRNAs are suppressed in mouse oocytes (11, 13). Oocyte activation relieved the suppressive state. Although ethanol treatment did not increase the miR-34c level (Fig. 1H) and did not affect Bcl-2 expression of the parthenogenetic oocytes (Fig. 5A, Middle), injection of precursor miR-34c significantly reduced the Bcl-2 protein level in parthenogenetic oocytes compared with levels in untreated oocytes and in oocytes injected with precursor-negative control. (Fig. 5B, Top and Middle). We also found lower Bcl-2 3'UTR reporter activities in parthenogenetic oocytes injected with precursor miR-34c (Fig. 5B, Bottom).

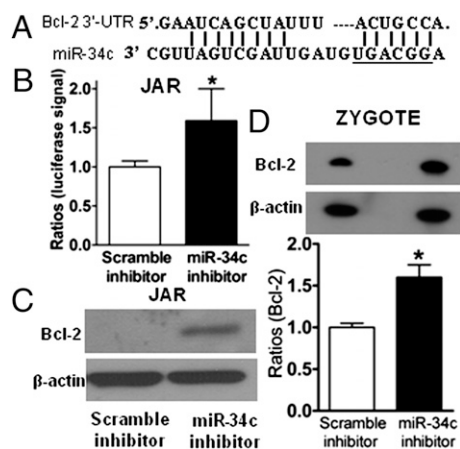


**Fig. 3.** Bcl-2 is a target of miR-34c. (A) Potential miR-34c-binding region on the 3' UTR of Bcl-2. The seed region of the miRNA is underlined. (B) The 3' UTR of Bcl-2 was cloned into reporter plasmid. The plasmid was transfected into JAR cells together with either miR-34c inhibitor or scramble inhibitor. Luciferase activity was significantly higher with the miR-34c inhibitor than with the scramble inhibitor ( $n = 4$ ). \* $P < 0.05$  with the scramble inhibitor. (C) Western blotting analysis showed that the expression Bcl-2 was elevated by inhibition of miR-34c in JAR cells.  $\beta$ -Actin was used as an internal control. (D) Western blotting analysis (Upper) and quantitation (Lower) of Bcl-2 protein in zygotes 6 h after injection of miR-34c inhibitor or scramble inhibitor. \* $P < 0.05$  with the scramble inhibitor.

## Discussion

Among the 25 miRNAs identified in the zona-bound sperm, 14 (let-7d, miR-16, -19b, -200b, -214, -221, -25, -30b, -30c, 3-0d, -342, -34c, -93, and -99a) are found in a panel of 54 miRNAs identified in the epididymal sperm (16). The miRNAs identified in this report are likely to be more representative of the miRNAs delivered to the oocyte during fertilization because zona pellucida binding is the first step in fertilization. This possibility is supported by (i) observations that miR-34c in the zona-bound sperm plays a role in the zygotic division; and (ii) lack of effect on pronuclear activation and preimplantation development after the coinjection into oocytes of sperm and inhibitors of some miRNAs found in epididymal sperm (16).

Our miRNA profiling supports previous findings on stage-specific expression of miRNAs in preimplantation embryos (6–8). Here we identify 16 zygotic miRNAs that could be important in early embryo development. These miRNAs were not found in previous studies, probably because of the use of different detection methods for miRNAs (6–9), different mouse strains (17), and embryos with or without culture (6, 8).

We tested the hypothesis that this unique set of zygotic miRNAs might be related to the first cleavage. The hypothesis is supported by the suppression of zygotic division and DNA synthesis with injection of the miR-34c inhibitor. Inhibition of DNA replication has long been known to arrest cleavage in one-cell embryos (18).

Three observations show that the zygotic miR-34c is derived from sperm: (i) Comparable levels of miR-34c were detected in the zona-bound sperm and zygotes but not in the oocytes; (ii) both the precursor and mature forms of miR-34c were present in sperm, and zygotes could convert precursor miR-212 to its mature form; and (iii)  $\alpha$ -amanitin treatment of oocytes did not reduce zygotic miR-34c. The contributions of the precursor and mature forms of sperm miR-34c to the formation of zygotic miR-34c remain to be determined.

Bcl-2 mediates the action of miR-34c on the first cleavage. Bcl-2 is a direct target of miR-34c, as shown by reporter assay and Western blotting in JAR cells and zygotes. The involvement of Bcl-2 in the first cleavage is consistent with the reported decrease in Bcl-2 mRNA expression in zygotes from 22 h after hCG injection to the two-cell stage (19–21).

Apart from its well-known antiapoptotic role, Bcl-2 has an antiproliferative function. In mouse, forced expression of Bcl-2 delays activation-induced T cells (22, 23), whereas Bcl-2 deficiency hastens (22) cell-cycle entry of T cells. The antiproliferative action of Bcl-2 is believed to act by elevating the expression of the negative cell-cycle regulator p27 and retarding S-phase entry (24, 25). Consistently, we observed an increase of p27 in embryos treated with the miR-34c inhibitor and failure of the inhibitor to inhibit

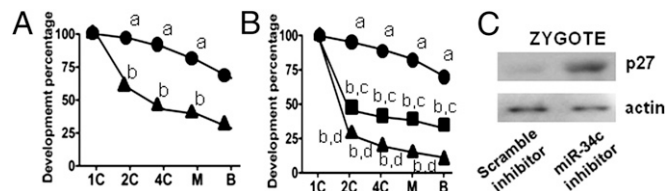


**Fig. 4.** Effects of Bcl-2 protein on embryo development. (A) One-cell (1C) zygotes were microinjected with Bcl-2 protein (▲) or water (●). Injection of Bcl-2 protein reduced the percentage of embryos reaching the two-cell (2C), four-cell (4C), morula (M), and blastocyst (B) stages. (B) Anti-Bcl-2 antibody partly rescued the inhibitory activity of the miR-34c inhibitor ( $n = 3$ ). Zygotes were microinjected with the miR-34c inhibitor (▲), Bcl-2 antibody (●), or both (■). Development percentage is based on the number of one-cell embryos used, which varied from 84–120 embryos. The letters "a," "b," "c," and "d" denote  $P < 0.009$  at the same time point. (C) Western blotting analysis indicates elevated expression of p27 in zygotes treated with the miR-34c inhibitor.

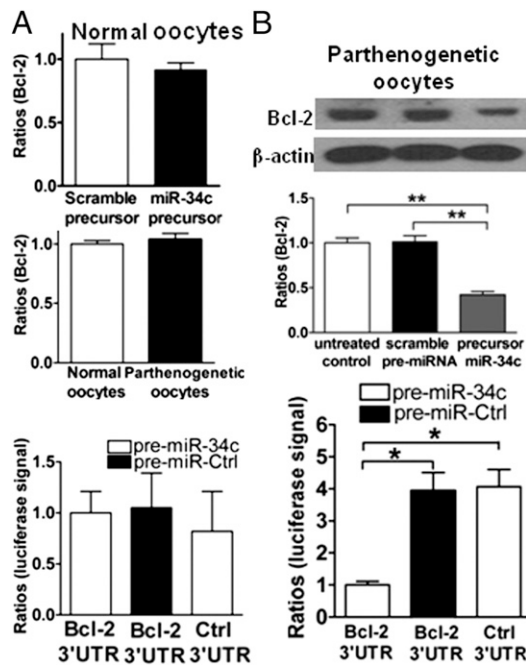


**Fig. 5.** MiR-34c function is suppressed in oocytes but not in parthenogenetic oocytes. (A) MiR-34c function is suppressed in oocytes as indicated by similar levels of Bcl-2 protein expression in oocytes injected with miR-34c precursor or scramble precursor (Top) and by the similar levels of luciferase activity in oocytes coinjected with miR-34c precursor and the Bcl-2 3' UTR luciferase reporter or control reporters (Bottom). Western blotting analysis shows no difference in Bcl-2 protein expression in normal and parthenogenetic oocytes (Middle), indicating that ethanol treatment does not affect the expression of Bcl-2 protein. (B) Western blotting analysis shows that injection of miR-34c precursor into parthenogenetic oocytes significantly suppresses Bcl-2 protein expression as compared with untreated parthenogenetic oocytes and oocytes injected with scramble miRNA precursor (Top and Middle). Coinjection of the precursor miR-34c (pre-miR-34c) and Bcl-2 3' UTR luciferase reporter constructs but not of scramble precursor miRNA (pre-miR-Ctrl) and control 3' UTR with mutated miR-34c-binding seed region (Ctrl 3' UTR) suppressed Bcl-2 3' UTR luciferase activity (Bottom). \* $P < 0.05$ ; \*\* $P < 0.001$ .

zygotic division 30 h after hCG injection, when DNA synthesis of the zygotes has been completed (26, 27). A dramatic decrease of p27 occurs after fertilization in mice (28), and p27 is increased in cleavage-arrested human embryos (29). Thus, it is likely that miR-34c exerts its effect on zygotic division by modulating Bcl-2 and p27. Bcl-2 also enhances F-actin polymerization (30), and dynamic changes in F-actin are important in fertilization and cleavage of zygotes (31). Whether Bcl-2-enhanced actin polymerization mediates the action of miR-34c on zygotic division is unknown.

Because anti-Bcl-2 antibody only partially rescues the suppressive effect of the miR-34c inhibitor, other miR-34c target genes were examined. The elevation of c-myc in zygotes treated with the miR-34c inhibitor suggests that miR-34c regulates zygotic c-myc. In mouse, c-myc expression increases after first cleavage (32). Whether c-myc mediates miR-34c-induced zygotic arrest remains to be determined.

*Dgcr8* is crucial to the production of miRNAs, and its deficiency is embryonically lethal in mice (12). However, *Dgcr8*-deficient oocytes can be fertilized with wild-type sperm and produce viable pups (11), demonstrating the importance of paternal miRNAs. The importance of sperm miR-34c on first cleavage shown here seems to contradict the observation that crosses between heterozygous males with female mice lacking maternal *Dgcr8* produce

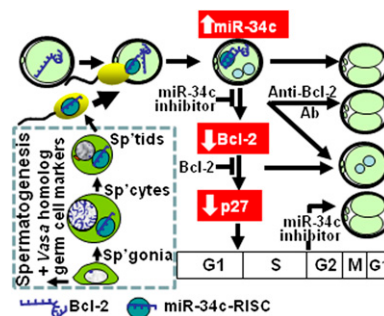


**Fig. 6.** Summary of the role of miR-34c in first cleavage. Meiosis in the testicular spermatogonia (Sp'gonia) leads to the formation of spermatocytes (Sp'cytes) and spermatids (Sp'tids), during which miR-34c is expressed in increasing amounts to enhance the expression of germ cell markers in the presence of Vasa homolog (14). The spermatids are transformed into sperm carrying miR-34c incorporating RNA-induced silencing complex (RISC). Upon fertilization, miR-34c-RISC is transferred from the sperm to the oocyte, reducing the expression of Bcl-2 and p27 and leading to S-phase entry and first cleavage. Inhibiting the process by injecting miR-34c inhibitor or recombinant Bcl-2 protein before S-phase inhibits first cleavage. Such treatment is not effective after S-phase and can be rescued partially by anti-Bcl-2 antibody.

a normal number of *Dgcr8*<sup>-/-</sup> blastocysts with the appropriate number of blastomeres (11). The discrepancy might result from the fact that spermatogenic cells are connected by intercellular cytoplasmic bridges that allow transfer of regulatory molecules among spermatogenic cells (33). Thus, *Dgcr8*-deficient sperm from heterozygous males could carry miRNAs or their precursors produced during spermatogenesis. In this connection, miR-34c is produced as early as the pachytene stage during spermatogenesis (14).

That the function of miR-34c is suppressed in the oocytes is consistent with previous reports (11, 13). The suppressed state is relieved after oocyte activation, as indicated by the miR-34c-induced reduction of reporter signal and Bcl-2 expression after ethanol treatment. The implication of zygotic miRNAs activation requires further investigation.

Ethanol-treated eggs cleave in the absence of sperm miR-34c. The observation might reflect differences in the mechanism of action in parthenogenetic activation and normal fertilization. The former fails to down-regulate inositol 1,4,5-trisphosphate receptor-1 to terminate calcium oscillation after fertilization (34, 35). The electrophysiology of the two types of activated oocytes is different also (36).

In summary, we provide evidence that sperm-borne miRNAs are delivered into the zygote during fertilization and that the paternal miR-34c is important for the first cleavage (Fig. 6). In addition to miRNAs, the fertilizing sperm also provide information influencing the first cleavage plane of the zygote (37), possibly by affecting the cytoskeletal dynamics (38). Further investigation is needed to identify the importance of sperm-derived factors, including other zygotic miRNAs, in the development of preimplantation embryos.

## Materials and Methods

**Sample Preparation.** The protocol for collecting oocytes, zygotes, and embryos was approved by the Committee on Use of Live Animals in Teaching and Research, the University of Hong Kong. For detailed descriptions of RNA extraction and miRNA profiling, please see *SI Materials and Methods*.

**Functional Analysis.** The details of zygote injection, BrdU incorporation, luciferase reporter assay, coimmunoprecipitation of the miRNA-Ago2 complex, and sperm transduction are described in *SI Materials and Methods*.

1. Krawetz SA (2005) Paternal contribution: New insights and future challenges. *Nat Rev Genet* 6:633–642.

2. Wu AT, et al. (2007) PAWP, a sperm-specific WW domain-binding protein, promotes meiotic resumption and pronuclear development during fertilization. *J Biol Chem* 282:12164–12175.

3. Dadoune JP (2009) Spermatozoal RNAs: What about their functions? *Microsc Res Tech* 72:536–551.
4. Ostermeier GC, Miller D, Huntriss JD, Diamond MP, Krawetz SA (2004) Reproductive biology: Delivering spermatozoan RNA to the oocyte. *Nature* 429:154.
5. Rassoulzadegan M, et al. (2006) RNA-mediated non-Mendelian inheritance of an epigenetic change in the mouse. *Nature* 441:469–474.
6. Yang Y, et al. (2008) Determination of microRNAs in mouse preimplantation embryos by microarray. *Dev Dyn* 237:2315–2327.
7. Tang F, et al. (2007) Maternal microRNAs are essential for mouse zygotic development. *Genes Dev* 21:644–648.
8. Viswanathan SR, et al. (2009) microRNA expression during trophoblast specification. *PLoS ONE* 4:e6143.
9. Ohnishi Y, et al. (2010) Small RNA class transition from siRNA/piRNA to miRNA during pre-implantation mouse development. *Nucleic Acids Res* 38:5141–5151.
10. Bernstein E, et al. (2003) Dicer is essential for mouse development. *Nat Genet* 35:215–217.
11. Suh N, et al. (2010) MicroRNA function is globally suppressed in mouse oocytes and early embryos. *Curr Biol* 20:271–277.
12. Wang Y, Medvid R, Melton C, Jaenisch R, Blelloch R (2007) DGCR8 is essential for microRNA biogenesis and silencing of embryonic stem cell self-renewal. *Nat Genet* 39:380–385.
13. Ma J, et al. (2010) MicroRNA activity is suppressed in mouse oocytes. *Curr Biol* 20:265–270.
14. Bouhallier F, et al. (2010) Role of miR-34c microRNA in the late steps of spermatogenesis. *RNA* 16:720–731.
15. Moore GD, Ayabe T, Kopf GS, Schultz RM (1996) Temporal patterns of gene expression of G1-S cyclins and cdk's during the first and second mitotic cell cycles in mouse embryos. *Mol Reprod Dev* 45:264–275.
16. Amanai M, Brahmajoyula M, Perry AC (2006) A restricted role for sperm-borne microRNAs in mammalian fertilization. *Biol Reprod* 75:877–884.
17. Byrne MJ, Warner CM (2008) MicroRNA expression in preimplantation mouse embryos from Ped gene positive compared to Ped gene negative mice. *J Assist Reprod Genet* 25:205–214.
18. Schultz RM (1993) Regulation of zygotic gene activation in the mouse. *Bioessays* 15:531–538.
19. Jin XL, O'Neill C (2011) Regulation of the expression of proto-oncogenes by autocrine embryotropins in the early mouse embryo. *Biol Reprod* 84:1216–1224.
20. Exley GE, Tang C, McElhinny AS, Warner CM (1999) Expression of caspase and BCL-2 apoptotic family members in mouse preimplantation embryos. *Biol Reprod* 61:231–239.
21. Jurisicova A, Latham KE, Casper RF, Casper RF, Varmuza SL (1998) Expression and regulation of genes associated with cell death during murine preimplantation embryo development. *Mol Reprod Dev* 51:243–253.
22. Linette GP, Li Y, Roth K, Korsmeyer SJ (1996) Cross talk between cell death and cell cycle progression: BCL-2 regulates NFAT-mediated activation. *Proc Natl Acad Sci USA* 93:9545–9552.
23. Cheng N, et al. (2004) Bcl-2 inhibition of T-cell proliferation is related to prolonged T-cell survival. *Oncogene* 23:3770–3780.
24. Zinkel S, Gross A, Yang E (2006) BCL2 family in DNA damage and cell cycle control. *Cell Death Differ* 13:1351–1359.
25. Greider C, Chattopadhyay A, Parkhurst C, Yang E (2002) BCL-x(L) and BCL2 delay Myc-induced cell cycle entry through elevation of p27 and inhibition of G1 cyclin-dependent kinases. *Oncogene* 21:7765–7775.
26. Gamow EI, Prescott DM (1970) The cell life cycle during early embryogenesis of the mouse. *Exp Cell Res* 59:117–123.
27. Artus J, Cohen-Tannoudji M (2008) Cell cycle regulation during early mouse embryogenesis. *Mol Cell Endocrinol* 282:78–86.
28. Kohoutek J, Dvorák P, Hampl A (2004) Temporal distribution of CDK4, CDK6, D-type cyclins, and p27 in developing mouse oocytes. *Biol Reprod* 70:139–145.
29. Civico S, Agell N, Bachs O, Vanrell JA, Balasch J (2002) Increased expression of the cyclin-dependent kinase inhibitor p27 in cleavage-stage human embryos exhibiting developmental arrest. *Mol Hum Reprod* 8:919–922.
30. Ke H, et al. (2010) BCL2 inhibits cell adhesion, spreading, and motility by enhancing actin polymerization. *Cell Res* 20:458–469.
31. Sun QY, Schatten H (2006) Regulation of dynamic events by microfilaments during oocyte maturation and fertilization. *Reproduction* 131:193–205.
32. Zeng F, Schultz RM (2005) RNA transcript profiling during zygotic gene activation in the preimplantation mouse embryo. *Dev Biol* 283:40–57.
33. Hermo L, Pelletier RM, Cyr DG, Smith CE (2010) Surfing the wave, cycle, life history, and genes/proteins expressed by testicular germ cells. Part 4: Intercellular bridges, mitochondria, nuclear envelope, apoptosis, ubiquitination, membrane/voltage-gated channels, methylation/acetylation, and transcription factors. *Microsc Res Tech* 73:364–408.
34. Brind S, Swann K, Carroll J (2000) Inositol 1,4,5-trisphosphate receptors are down-regulated in mouse oocytes in response to sperm or adenophostin A but not to increases in intracellular Ca(2+) or egg activation. *Dev Biol* 223:251–265.
35. Jellerette T, He CL, Wu H, Parys JB, Fissore RA (2000) Down-regulation of the inositol 1,4,5-trisphosphate receptor in mouse eggs following fertilization or parthenogenetic activation. *Dev Biol* 223:238–250.
36. Eusebi F, Siracusa G (1983) An electrophysiological study of parthenogenetic activation in mammalian oocytes. *Dev Biol* 96:386–395.
37. Piotrowska K, Zernicka-Goetz M (2001) Role for sperm in spatial patterning of the early mouse embryo. *Nature* 409:517–521.
38. Gray D, et al. (2004) First cleavage of the mouse embryo responds to change in egg shape at fertilization. *Curr Biol* 14:397–405.

# Supporting Information

Liu et al. 10.1073/pnas.1110368109

## SI Materials and Methods

**Collection of Mouse Oocytes and Embryos.** Imprinting control region (ICR) female mice (age 6–8 wk) were superovulated by successive injections of 5 IU of pregnant mare serum gonadotropin (Sigma) and 5 IU of human chorionic gonadotropin (hCG; Sigma) 47–48 h apart and were mated with male mice. Unfertilized eggs were harvested 21 h after hCG injection. Pronucleated zygotes (one-cell embryos), two-cell, four-cell, eight-cell, and morulae-stage embryos were flushed from the oviducts 21/40/42, 54–56, 62–64, and 76–78 h after hCG injection, respectively. Blastocysts were retrieved from the uterine horns 86–88 h after hCG. Parthenogenetic activation was achieved by exposing oocytes to 7% ethanol (vol/vol) for 5 min at 37 °C. After activation, the oocytes were incubated for 4 h in amino acids-supplemented embryo culture medium (KSOM/AA, Chemicon) containing 0.5 µg/mL cytochalasin D.

**Extraction of Total RNA.** Embryos at the same developmental stage were pooled randomly into three groups with five embryos per group. Total RNA was extracted from each group in 0.5 µL of 2 M guanidine isothiocyanate (Sigma) at room temperature for 5 min. The completion of lysis was confirmed by microscopy. The samples were diluted to 5 µL with double-distilled water and were used directly for the multiplex microRNA (miRNA) assay.

**Reverse Transcription for miRNA Profiling.** The protocol for miRNA profiling involves three steps: reverse transcription, pre-PCR amplification, and quantitative real-time PCR (qPCR). The details of the procedures have been described previously (1). Briefly, reverse-transcription reactions were performed in a volume of 10 µL containing 1 µL of 10× cDNA archive kit buffer (Applied Biosystems), 100 U of Moloney murine leukemia virus reverse transcriptase, 5 mM of dNTP, 2.6 U of RNase inhibitor, and 50 nM of reverse-transcription primers for a total of 238 miRNAs, 3.425 mM of MgCl<sub>2</sub>, and 4.5 µL of total RNA. The reaction conditions were 16 °C for 30 min, followed by 60 cycles of 20 °C for 30 s, 42 °C for 30 s, and 50 °C for 1 s. Subsequently the enzyme was inactivated by incubation at 85 °C for 5 min.

For pre-PCR amplification, the cDNAs obtained were pre-amplified in 50 µL of pre-RT-PCR mixture containing 25 µL of 2× TaqMan Universal Master Mix with no AmpErase uracil *N*-glycosylase (UNG) (Applied Biosystems), 10 µL of cDNA product, 50 nM of 238-plex forward primer for each miRNA, 5 nM of universal reverse primer, 12.5 U of AmpliTaq Gold, 2 mM of dNTP, 2 mM of MgCl<sub>2</sub>, and 3 µL of double-distilled water. The conditions for PCR were 95 °C for 10 min, 55 °C for 2 min, followed by 18 cycles of 95 °C for 1 s and 65 °C for 1 min.

For PCR analysis, 50 µL of the preamplified sample was diluted to 300 µL by adding 250 µL of water. Real-time PCR mixtures contained 5 µL of 2× Universal Master Mix with no AmpErase UNG (Applied Biosystems), 0.5 µM of forward primer and 1 µM of TaqMan probe mixture, 1 µM of universal reverse primer, 1 µL of diluted preamplified RT-PCR sample, and 0.9 µL of double-distilled water. The conditions used were as follows: 95 °C for 10 min, followed by 40 cycles at 95 °C for 15 s, and 60 °C for 1 min. All the reactions were analyzed in an ABI 7500 Real-time PCR System. A cycle threshold (Ct) value <26 was considered as an expression level twofold higher than the sensitivity of the assay.

**Quantitative RT-PCR for Precursor and Mature Forms of miR-34c.** In each analysis, five zona-bound spermatozoa, five oocytes, and five zygotes were collected and subjected to RNA extraction. Residual

genomic DNA was digested by TUBRO DNase (Ambion) for 30 min at 37 °C. Reverse transcription and assays for precursor miR-34c were performed using the TaqMan Reverse Transcription kit and TaqMan Pri-miRNA assays (Applied Biosystems) according to the manufacturer's instruction.

Quantitative RT-PCRs of mature miRNA were performed by TaqMan miRNA assays. Briefly, the embryos were collected and treated as above. Reverse transcription was performed using the TaqMan miRNA reverse transcription kit (Applied Biosystems). Quantitative real-time PCR was performed using the Real-time PCR System (Applied Biosystems). The condition for PCR was 95 °C for 10 min, followed by 40 cycles of 95 °C for 15 s and 60 °C for 1 min.

**Injection of Zygotes.** Fertilized one-cell zygotes were collected 20–22 h after hCG injection. About 10 pL of 25-µM miR-34c inhibitor or scramble inhibitor (Exiqon) was injected into the cytoplasm of the zygotes using a micromanipulator (Narishige). Groups of 20–30 injected embryos were cultured for 4 d in potassium simplex optimized medium with amino acids (KSOM/AA) overlaid with mineral oil at 37 °C in 5% CO<sub>2</sub>. The concentrations of recombinant Bcl-2 protein (R&D Systems) and anti-Bcl-2 antibody (Santa Cruz Biotechnology) were adjusted to 32 µM and 100 ng/µL, respectively, before injection.

**Sperm miRNA Transduction and in Vitro Fertilization.** Mouse spermatozoa were transduced with precursor by using the Bio-PORTER QuikEase protein delivery kit (Sigma) according to the manufacturer's instructions. Briefly, 100 pmoles of precursor miRNA molecules were dissolved in M199 medium (Sigma) and mixed with the QuikEase transduction agent (Sigma). The mixture was used to transduce  $0.5 \times 10^6$  spermatozoa for 2.5 h at 37 °C. After transduction, the spermatozoa were collected by centrifugation and washed three times before insemination. After the last washing, the M199 medium was replaced with human tubal fluid (HTF) medium (Millipore). Superovulated oviductal cumulus-oocyte masses were collected 13 h after hCG administration for in vitro fertilization. Fertilized zygotes as evidenced by the presence of two pronuclei were collected at 8 h after insemination and were washed extensively before quantitative RT-PCR (qRT-PCR) assays.

**In Vitro Fertilization and  $\alpha$ -Amanitin Treatment of Embryos.** Unfertilized oocytes were collected from superovulated ICR mice. Sperm were collected from the caudal epididymis of mature ICR mice. The oocytes were incubated with medium containing 25 µg/mL of  $\alpha$ -amanitin (2) 30 min before, during, and after insemination.

**BrdU Incorporation Assay.** DNA synthesis was determined by BrdU incorporation assays. Briefly, the zygotes were cultured in KSOM medium containing 100 µM of BrdU for 30 min before washing with PBS. After removal of the zona pellucida, the zygotes were fixed at –20 °C in 100% methanol for 20 min and were permeated in PBS containing 1% BSA and 0.1% Triton X-100; then DNA was denatured in 4N HCl for 30 min. The incorporated BrdU was detected by incubation with primary monoclonal antibody against BrdU (1:100 dilution; Thermo Scientific) for 1 h at 37 °C, followed by staining with FITC-conjugated anti-mouse IgG (1:100 dilution; Invitrogen) for another hour at 37 °C. The fluorescence signal was visualized under a Nikon TE300 inverted microscope (Nikon).

**Luciferase Reporter Assays.** The potential Bcl-2 3' UTR miR-34c-binding sequence (171–218 of the 3' UTR) was subcloned to the

NotI/XhoI sites of the psiCheck-2 vector (Promega). The primers used are listed below. The vector was transfected together with either the miR-34c inhibitor or scramble inhibitor into a trophoblast cell line, JAR (America Type Culture Collection), by Lipofectamine 2000 (Invitrogen). After 24 h the cells were lysed, and luciferase activity assays were performed with the Dual-Luciferase Reporter Assay System (Promega). Luciferase signal was measured by the Glomax luminometer (Promega). Renilla luciferase (hRluc) activity was normalized by the synthetic firefly luciferase (hluc<sup>+</sup>) activity as an internal control.

To enhance the sensitivity of the assays in oocytes, two copies of the potential Bcl-2 miR-34c-binding site/mutant-binding sites (amino acids 184–206 of the 3' UTR) were cloned to the NotI/XhoI sites downstream of the hRluc gene of the psiCheck-2 vector (Promega). To generate the mutants, the seed-binding region of the Bcl-2 3' UTR was mutated to abolish miR-34c-binding. To synthesize RNAs for microinjection, plasmid templates were prepared by cutting with NotI (New England Biolabs). The 5'-capped RNA was synthesized using the mMessage mMachine kit (Ambion). Residual DNA templates were removed by digestion with DNase. A poly-A tail was added to the RNA by using the Poly (A) Tailing kit (Ambion). The quality of the synthesized RNA was assessed on a denatured RNA gel. The hluc<sup>+</sup> gene was released from the psiCheck-2 vector (Promega) by digestion with EcoRI/BamHI (New England Biolabs) and was subcloned into the pRC-CMV vector (Invitrogen). To generate RNA for microinjection, the vector was digested with NotI, and RNA was synthesized as above. The reporters, control hluc<sup>+</sup>, and precursor miRNAs were mixed and microinjected into zygotes at a molar ratio of 3:1:9. The embryos were lysed 24 h after microinjection. The luciferase activities were measured and normalized as above.

The following primers were used to generate miR-34c reporter constructs:

For constructs used in cell line:

Bcl2-F: tcgag ttcaggcaaatggtcgaatcagctatttactgccaagggaatcagc

Bcl2-R: ggccgctgatatttcccttggcagtaaatagctgattgaccatttggcgaac

For constructs used for oocyte microinjection:

Bcl2 × 2-F: tcgagtcgaatcagctatttactgccaagctatcgaatcagctatttactgccaagc

Bcl2 × 2-R: ggccgcttggcagtaaatagctgattcgaatgcttggcagtaaatgctgattcgc

Mutant primers:

Bcl2 × 2M-F: tcgagtcgaatcagctatttgcggaagctatcgaatcagctatttgcggaagc

Bcl2 × 2M-R: ggccgcttccgtaaatagctgattcgaatgcttccgtaaatagctgattcgc

The potential miR-34c-binding regions are underlined on the sense strand. Mutated binding sites are in italics. When multiple

copies of the potential binding sites were used, a linked was added to separate the regions (labeled in bold).

**Western Blot Analysis.** Embryos at different stages were rinsed twice in PBS, resuspended in 10  $\mu$ L of Laemmli buffer, and boiled for 10 min. The samples were run on 10% SDS/PAGE gels and transferred onto nitrocellulose membranes, which were incubated with the primary antibodies overnight at 4 °C in Tris-buffered saline with 0.5% Tween 20 (Sigma) (TBST) containing 5% nonfat milk; followed by incubation with appropriate secondary antibody conjugated to HRP (1:1,000) in TBST for 1 h. The bands were detected using an ECL kit (Santa Cruz).

**Coimmunoprecipitation of Sperm miRNA–Argonaute 2 Protein Complex.** Coimmunoprecipitation of miR-34c and argonaute 2 (Ago2) was performed as reported (3). Briefly, mouse spermatozoa were collected from the caudal epididymis of mature mice, washed three times with M199 containing 0.4% BSA, capacitated, and allowed to swim up for 1.5 h. The active spermatozoa were collected, washed twice with M199 without BSA, and lysed in ice-cold radioimmunoprecipitation assay lysis buffer [20 mM Tris-HCl (pH 7.5), 150 mM NaCl, 1 mM EDTA, 1% Nonidet P-40, 1% sodium deoxycholate, 2.5 mM sodium pyrophosphate, and 1  $\mu$ g/mL leupeptin] for 15 min. Debris was removed by centrifugation, and the supernatant was diluted with PBS and cleared by shaking incubation with protein G beads (GE Healthcare) and 2  $\mu$ g of normal rabbit IgG for 3 h at 4 °C. The cleared lysate then was incubated with ChIP-grade anti-Ago2 antibody (Abcam) at 4 °C overnight with shaking. The Ago2 protein complexes were collected by protein G beads with extensive washing the next day. The presence of miR-34c in the complexes was determined by qRT-PCR assay after the beads were boiled in diethyl pyrocarbonate-treated water for 3 min.

**Data Analysis.** Statistical analyses of miRNA profiling data were performed with the GeneSpring software version 7.3 (Sigenetics) based on their Ct values. The miRNAs were grouped into six groups according to the mean values. A one-way ANOVA non-parametric *t* test was applied. The Benjamini–Hochberg multiple testing correction was used to control the false-discovery rate. A *P* value <0.05 was used to define a set of significantly up- and down-regulated genes. Hierarchical clustering analysis was performed based on the filtered genes that met the statistical criteria as above. Values for each miRNA were median-centered before clustering. For qRT-PCR analysis, the  $\Delta$ Ct method was used to calculate the relative expression levels in the experimental group and the control group. For experiments other than miRNA profiling, the differences between the control and the experimental groups were analyzed by the Mann–Whitney test. For multiple group comparisons, one-way ANOVA was applied. Differences were considered statistically significant at *P* < 0.05. All reported results are based on at least three independent observations.

1. Tang F, et al. (2007) Maternal microRNAs are essential for mouse zygotic development. *Genes Dev* 21:644–648.  
2. Liu H, Kim JM, Aoki F (2004) Regulation of histone H3 lysine 9 methylation in oocytes and early pre-implantation embryos. *Development* 131:2269–2280.

3. Ikeda K, et al. (2006) Detection of the argonaute protein Ago2 and microRNAs in the RNA induced silencing complex (RISC) using a monoclonal antibody. *J Immunol Methods* 317:38–44.

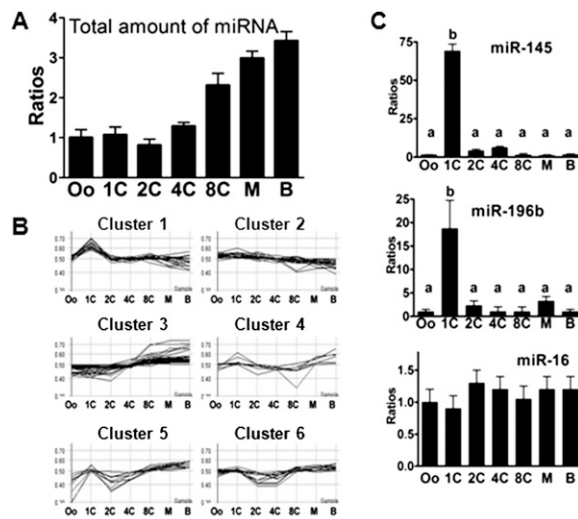


**Fig. 51.** miRNA expression in gametes and preimplantation mouse embryos. (A) Global changes in miRNA expression of mouse embryos during preimplantation development. The total amount of miRNA expression in embryos is expressed as the ratio to that in oocytes (Oo) and at the one-cell (1C), two-cell (2C), four-cell (4C), eight-cell (8C), morula (M), and blastocyst (B) stages. (B) *k*-means clustering of miRNAs in preimplantation embryos. Temporal expression profiles of 94 miRNAs were analyzed by *k*-means clustering. The analysis divided the miRNAs into six clusters based on similarities in expression profiles throughout the preimplantation period. The miRNAs in each cluster are presented in Dataset S1. (C) Validation of miRNA expression by qRT-PCR without preamplification of miRNA in preimplantation mouse embryos. The expression levels of miR-145, -196b, and -16 at different developmental stages were quantified by quantitative PCR on pooled embryos ( $n = 5$ ). All the values were calculated against oocyte Ct values and therefore are represented as relative fold-change against oocyte miRNAs [ $2^{-(Ct_{\text{oocyte}} - Control_x)}$ ]. All data were normalized by endogenous RNA U6 expression. The letters "a" and "b" above the bars denote significant differences ( $P < 0.05$ ) between groups.

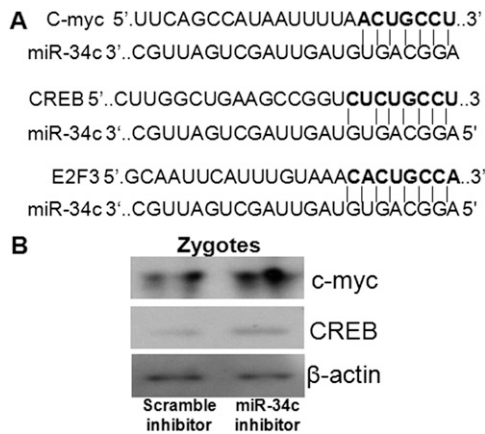


**Fig. 52.** Potential miR-34c targets in zygotes. (A) Potential miR-34c-binding region on the 3' UTRs of c-myc, cAMP response element-binding (CREB), and E2F3. The seed-binding region of the 3' UTRs is in bold. (B) Western blotting analysis of potential miR-34c targets in zygotes 6 h after injection with miR-34c inhibitor or scramble inhibitor.

